W. T. Weeks L. L. Wu M. F. McAllister A. Singh

Resistive and Inductive Skin Effect in Rectangular Conductors

A model based on network theory is presented for calculating the frequency-dependent resistance and inductance per unit length matrices for transmission line systems consisting of conductors with rectangular cross sections. The calculated results are compared with actual measurements. Excellent agreement is obtained over a wide range of frequencies, including the mid-range where neither dc values nor high-frequency limit values apply.

Introduction

Modern technology has shown a relentless trend towards faster circuits, shorter rise times, and smaller pulse widths. Simultaneously, the geometric dimensions of modern circuit packages have been shrinking. It is fairly typical that the widths and thicknesses of intercircuit wiring closely approximate the skin depths for non-negligible frequency components in the pulses to be transmitted. This greatly complicates the electrical analysis of packages. For the frequency range in question, the actual wiring resistance may be much higher than the dc resistance. Alternatively, the significant frequencies may be too low to use the traditional high-frequency approximations, which predict a skin resistance and inductance proportional to the square root of frequency. The accurate calculation of resistance and inductance through this relatively unexplored mid-range of frequencies is the subject of this paper. The frequency-dependent impedance per unit length matrix will be obtained for a transmission line system consisting of conductors with rectangular cross sections.

At very low frequencies, current distributes itself uniformly throughout the cross section of a conductor. As the frequency increases, the current redistributes, crowding towards the surface of the conductor until, at very high frequencies, it is effectively confined to a thin skin

just inside the surface of the conductor. The determination of the current density as a function of frequency is the major problem in developing a theory of skin effect.

Analytical methods, even approximate ones, are quite limited. An excellent survey of the state of the art has been given by Casimir and Ubbink [1]. Numerical methods tend to be more flexible, permitting analysis of systems of more than one conductor and of conductors having a wide variety of cross sections. Silvester [2] has described a method in which the current density is obtained as an eigenfunction expansion, where each eigenfunction represents an independent current density mode which must be determined numerically. Silvester obtained excellent agreement with measurements of the resistance of a rectangular bar. Popović and Popović [3] and Popović and Filipović [4] have obtained the current density as an approximate solution to an integral equation. They calculate skin resistance from the average power dissipated in the conductors.

A coupled circuit theory approach has been taken by Graneau [5, 6]. Graneau proceeds by dividing each conductor into segments which run the length of the conductor but have small cross-sectional areas. The resistance and inductance of each segment and the mutual in-

Copyright 1979 by International Business Machines Corporation. Copying is permitted without payment of royalty provided that (1) each reproduction is done without alteration and (2) the *Journal* reference and IBM copyright notice are included on the first page. The title and abstract may be used without further permission in computer-based and other information-service systems. Permission to republish other excerpts should be obtained from the Editor.

ductance between segments are calculated and the coupled circuit equations set up. Segment currents are obtained as power series expansions in frequency. With trivial modifications, Graneau's method can be adapted to the calculation of the impedance per unit length matrix for a transmission line system. Each matrix element can be obtained as a ratio of power series expansions in frequency. Graneau's formulation is essentially the same as the one used in this paper. The solution methods, however, differ dramatically. The formulation to be given avoids the use of series expansions.

A partial element equivalent circuit method for calculating current distributions in three-dimensional multiconductor systems has been described by Ruehli [7, 8]. This method has been applied by Ruehli, Kulasza, and Pivnichny [9] to obtain the frequency-dependent resistance and inductance of an L-shaped conductor.

In the present paper, an explicit calculation of the current density is avoided altogether. The conductors are divided into parallel segments having small, rectangular cross sections. The current density is assumed to be constant throughout a segment, but is allowed to vary from segment to segment so that, in principle, a step function approximation to the current density is obtained. The dc resistance and self-inductance of each segment and the mutual inductance between all segments are calculated, and the impedance per unit length matrix for the collection of segments is set up. The impedance per unit length matrix for the system of conductors is obtained by forming appropriate row and column sums over the segment matrix, so that an explicit calculation of the segment currents is bypassed. Theoretical development will be limited to systems of parallel conductors having rectangular cross sections, but can be generalized easily to conductors having arbitrary cross sections.

Theoretical development

The calculation is begun by subdividing each conductor into parallel segments having small cross-sectional areas as shown in Fig. 1. Let the conductors be numbered from 0 to N in such a manner that conductor 0 is the ground conductor, and the remaining N conductors are the active conductors. Now divide the ith active conductor into N_i segments ($i = 1, 2, \dots, N$). Divide the ground conductor 0 into $N_0 + 1$ segments, selecting one segment near the center of the conductor as a reference segment. The segments will be labeled as follows:

- (i, j) refers to the jth segment of the ith conductor. Here, $j = 1, 2, \dots, N$, while $i = 0, 1, 2, \dots, N$.
- (0, 0) refers to the reference segment on the ground conductor.

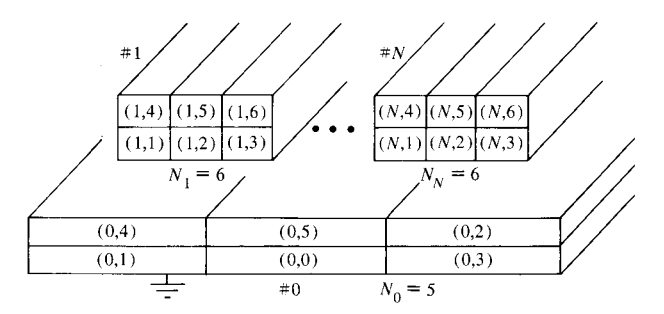


Figure 1 Division of conductors into segments.

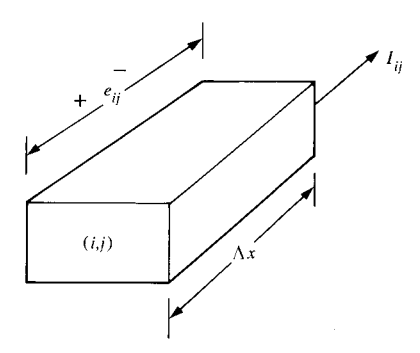


Figure 2 Current-voltage relationship of a length Δx of segment (i, j).

There are M + 1 conductor segments, where

$$M = \sum_{i=0}^{N} N_i; \tag{1}$$

M is the total number of segments not including the reference segment.

Taking the x-axis parallel to the long dimension of the collection of conductor segments, consider a section of length Δx as shown in Fig. 2. Let

 e_{ij} = voltage drop across a length Δx of segment (i, j), (2)

$$I_{ii}$$
 = current through segment (i, j) . (3)

It is assumed that all current flow is in the direction of the x-axis, i.e., that current enters and leaves the end faces of a segment but does not flow across the sides of the segment.

The purpose of dividing each conductor into segments is to approximate the current density in the conductors. It will be assumed that the current density is uniform and

653

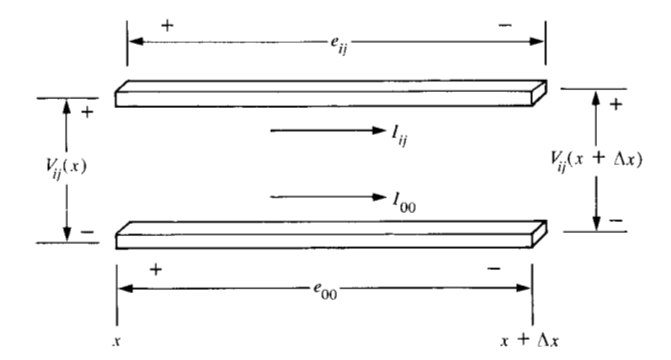


Figure 3 Voltage relationships between segment (i, j) and the reference segment.

constant within a segment but varying from segment to segment, so that one obtains a step function approximation of the actual current density within the conductors.

Assuming there is a uniform and constant density within each segment, one has

$$r_{ij} = \frac{1}{\sigma_i A_{ij}} \tag{4}$$

for the dc resistance per unit length of segment (i, j). Here, σ_i is the conductivity of conductor i, and A_{ij} is the cross-sectional area of segment (i, j). Under the same assumptions, the partial inductance per unit length between segments (i, j) and (k, m) is given by

$$L_{ij,km}^{(p)} = -\frac{\mu}{4\pi A_{ij} A_{km}} \iiint \ln [(y - y')^{2} + (z - z')^{2}] dy' dz' dy dz,$$
(5)

where the integration over y and z is taken over the cross section of segment (i, j), and the integration over y' and z' is taken over the cross-sectional area of segment (k, m). For segments having rectangular cross sections, the multiple integral in Eq. (5) can be evaluated in closed form by observing that if

$$F(y, z) = \left(\frac{y^4 - 6y^2z^2 + z^4}{24}\right) \ln (y^2 + z^2)$$
$$-\frac{yz}{3} \left(y^2 \tan^{-1} \frac{z}{y} + z^2 \tan^{-1} \frac{y}{z}\right),$$

then

$$\frac{\partial^4 F(y-y',z-z')}{\partial y \partial z \partial y' \partial z'} = -\ln \left[(y-y')^2 + (z-z')^2 \right] - \frac{25}{6} .$$

Thus, the evaluation of the multiple integral reduces to 16 evaluations of the function F(y - y', z - z'), with y, z and y', z', respectively, taking on values at the vertices of segments (i, j) and (k, m).

The derivation of Eq. (5), starting from the expression for the energy stored in the magnetic field, requires that the sum of the currents through all the conductor segments be zero; otherwise, the replacement of volume integrals by surface integrals would be impossible because of the logarithmic nature of the vector potential.

The voltages e_{ij} and currents I_{ij} are related by the equations

$$e_{ij} = \sum_{k=0}^{N} \sum_{m=1}^{N_k} (r_{ij} \delta_{ik} \delta_{jm} + \hat{j} \omega L_{ij,km}^{(p)}) I_{km} \Delta x + \hat{j} \omega L_{ij,00}^{(p)} I_{00} \Delta x$$
(6)

and

$$e_{00} = (r_{00} + \hat{j}\omega L_{00,00}^{(p)})I_{00}\Delta x + \hat{j}\omega \sum_{k=0}^{N} \sum_{m=1}^{N_k} L_{00,km}^{(p)}I_{km}\Delta x,$$
 (7)

where $\delta_{ii} = 1$, $\delta_{ij} = 0$ when $i \neq j$, and \hat{j} is the square root of -1. The index j takes on values $j = 1, 2, \dots, N_i$, while $i = 0, 1, \dots, N$.

There are M + 1 equations, one for each of the M + 1 segments, including the reference segment (0, 0).

It was pointed out above that in order for Eq. (5) to be valid, it is necessary that the sum of the currents in the system of conductor segments be zero. This condition is fulfilled by requiring that

$$I_{00} = -\sum_{i=0}^{N} \sum_{j=1}^{N_i} I_{ij}.$$
 (8)

Substituting Eq. (8) into Eqs. (6) and (7) and dividing by Δx yields

$$\frac{e_{ij}}{\Delta x} = \sum_{k=0}^{N} \sum_{m=1}^{N_k} \left[r_{ij} \delta_{ik} \delta_{jm} + \hat{j} \omega (L_{ij,km}^{(p)} - L_{ij,00}^{(p)}) \right] I_{km},$$
(9)

$$\frac{e_{00}}{\Delta x} = \sum_{k=0}^{N} \sum_{m=1}^{N_k} \left[-r_{00} + \hat{j}\omega (L_{00,km}^{(p)} - L_{00,00}^{(p)}) \right] I_{km}.$$
 (10)

In transmission line theory, it is convenient to introduce the voltage drop from a conductor to the reference conductor at a fixed position x along the length of the line. Thus, let

 $V_{ii}(x)$ = voltage of segment (i, j)

with respect to (0, 0) at position x.

Referring to Fig. 3, one sees that

$$e_{00} + V_{ii}(x) = V_{ii}(x + \Delta x) + e_{ii}$$

from which it follows that

$$-\Delta V_{ij} = V_{ij}(x) - V_{ij}(x + \Delta x) = e_{ij} - e_{00}.$$
 (11)

654

If Eq. (10) is subtracted from Eq. (9), and Eq. (11) is used to eliminate $e_{ij} - e_{00}$, the result is

$$-\frac{\Delta V_{ij}}{\Delta x} = \sum_{k=0}^{N} \sum_{m=1}^{N_k} [R_{ij,km} + \hat{j}\omega L_{ij,km}] I_{km},$$
 (12)

where

$$R_{ij,km} = r_{00} + r_{ij}\delta_{ik}\delta_{im}, \tag{13}$$

$$L_{ij,km} = L_{ij,km}^{(p)} - L_{ij,00}^{(p)} - L_{00,km}^{(p)} + L_{00,00}^{(p)};$$
 (14)

or, if one defines

$$Z_{ij,km} = R_{ij,km} + \hat{j}\omega L_{ij,km},\tag{15}$$

the

$$-\frac{\Delta V_{ij}}{\Delta x} = \sum_{k=0}^{N} \sum_{m=1}^{N_k} Z_{ij,km} I_{km},$$
 (16)

where $i = 0, 1, 2, \dots N$ and $j = 1, 2, \dots, N_i$. The matrix **Z**, defined by Eq. (15), is an $M \times M$ matrix, where M is given in Eq. (1). That is, the order of **Z** is one less than the total number of conductor segments. Generally, this order should be as large a number as possible.

The next step of the computation is to invert the matrix **Z** of Eq. (15) to get

$$\mathbf{Y} = \mathbf{Z}^{-1}.\tag{17}$$

With the aid of the inverse, Eq. (16) can be solved for I_{ij} . Thus

$$I_{ij} = -\sum_{k=0}^{N} \sum_{m=1}^{N_k} Y_{ij,km} \frac{\Delta V_{km}}{\Delta x} .$$
 (18)

Now the total current in conductor i is the sum of the currents in each of its N_i segments. Thus,

$$I_{i} = \sum_{j=1}^{N_{i}} I_{ij} \tag{19}$$

is the total current in the *i*th conductor. Summing Eq. (18) over j and using Eq. (19), one obtains

$$I_{i} = -\sum_{k=0}^{N} \sum_{j=1}^{N_{i}} \sum_{m=1}^{N_{k}} Y_{ij,km} \frac{\Delta V_{km}}{\Delta x}.$$
 (20)

It will be assumed that conductor cross sections perpendicular to the x-axis are equipotential surfaces; that is, the voltage drop e_{ij} across any segment (i, j) is the same as the voltage drop e_{ij} across any other segment (i, j') on the same conductor. In other words, it is assumed that e_{ij} depends only on the conductor index i and not on the segment index j where $j = 1, 2, \dots, N_i$. This, of course, is an approximation, but probably a very good one. This assumption, along with the defining equation (11), implies that

$$\Delta V_{0i} = 0$$
 $j = 1, 2, \dots, N_0,$ (21a)

$$\Delta V_{ii} = \Delta V_{ii'}$$
 $j, j' = 1, 2, \dots, N_i$. (21b)

From Eq. (21b) it follows that one can write

$$\Delta V_{ii} = \Delta V_i \qquad j = 1, 2, \cdots, N_i. \tag{22}$$

Consequently, Eq. (20) can be written as

$$I_i = -\sum_{k=1}^{N} y_{ik} \frac{\Delta V_k}{\Delta_r}, \tag{23}$$

where

$$y_{ik} = \sum_{i=1}^{N_i} \sum_{m=1}^{N_k} Y_{ij,km}.$$
 (24)

The matrix y of Eq. (24) is an $N \times N$ matrix and generally N is much smaller than M.

Now invert the matrix y, defined by Eq. (24), to get the $N \times N$ matrix

$$\mathbf{z} = \mathbf{v}^{-1}.\tag{25}$$

With the aid of the inverse, Eq. (23) may be solved for $\Delta V_{\nu}/\Delta x$ to get

$$-\frac{\Delta V_i}{\Delta x} = \sum_{k=0}^{N} \mathbf{z}_{ik} \mathbf{I}_k. \tag{26}$$

Equation (26) approximates the familiar transmission line equation

$$-\frac{dV_i}{dx} = \sum_{k=0}^{N} \mathbf{z}_{ik} I_k.$$

The accuracy of the approximation should improve as the number of segments M is increased.

In order to obtain accurate results, the conductors should be divided into segments whose dimensions are no greater than the skin depth

$$\delta = \left(\frac{2}{\mu\sigma\omega}\right)^{1/2}$$

at the angular frequency ω under consideration. At high frequencies this may be impractical. The total number of segments M is the dimension of the complex impedance matrix \mathbf{Z} of Eq. (15). The maximum value of M is limited by the amount of storage available in the computer system being used for the analysis. Values of M larger than 700 are probably impractical for most present-day systems.

The following rule for dividing conductors into segments seems to work quite well. Let W be the width and T be the thickness of a conductor. Let n and m be the number of subdivisions into which the width and thickness, respectively, are to be divided to obtain nm segments. Let ΔW and ΔT be the dimensions of a segment. Then,

655

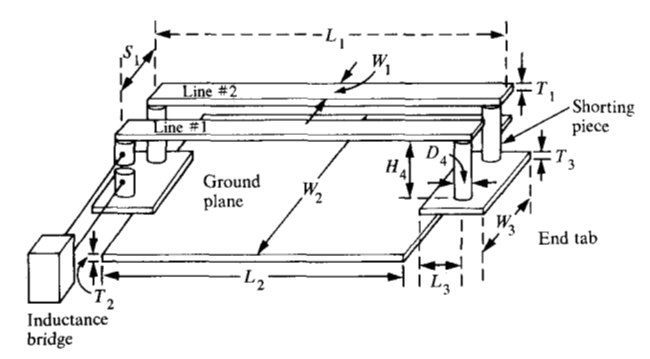


Figure 4 Simplified drawing of experimental setup with both striplines in place.

Table 1 Dimensions of the model shown in Fig. 4.

Striplines	Width	$W_1 = 0.952 \text{cm}$
-	Thickness	$T_1^{1} = 0.368$
	Length Center-to-center	$L_1 = 125.88$
	separation	$S_1 = 5.08$
Ground planes	Width	$W_2 = 52.07$
	Thickness	$T_2^2 = 0.0940$
	Length	$L_2^2 = 122.52$
End tabs	Width	$W_3 = 13.97$
	Thickness	$T_3^3 = 0.119$
	Length	$L_3 = 1.683$
Shorting pieces	Diameter	$D_4 = 2.223$ $H_4 = 4.21$
	Height	$H_4 = 4.21$

- 1. If $W/n \le \delta$ choose $\Delta W = W/n$.
- 2. If $W/n > \delta$, then
 - a. If n = 2k + 2 choose $\Delta W = \delta$ for the 2k outermost divisions and $\Delta W = (W/2) k\delta$ for the two center divisions.
 - b. If n = 2k + 1 choose $\Delta w = \delta$ for the 2k outermost divisions and $\Delta W = W 2k\delta$ for the center division.

To calculate ΔT , replace W with T and n with m in the above rule. Simply put, at high frequencies the segments are chosen in layers one skin depth deep, starting from the conductor surfaces, leaving a core of one, two, or four large segments near the center of the conductor.

The computational procedure can be summarized as follows:

- Divide the conductors into segments according to the rule described above.
- Calculate the resistance of each segment, using Eq. (4).

- 3. Calculate the matrix of partial inductances, using Eq. (5).
- 4. Use Eqs. (13) through (15) to calculate the complex matrix \mathbf{Z} at the angular frequency ω .
- 5. Invert the matrix Z to obtain the matrix Y.
- 6. Add the rows and the columns of Y, as indicated in Eq. (24), to obtain the matrix y.
- 7. Invert y to obtain the desired impedance per unit length matrix z.

The procedure is to be repeated for each frequency of interest.

The limitation of the derivation to systems of conductors having rectangular cross sections is somewhat artificial. Conceptually, the theory is easily generalized to conductors having arbitrary cross sections. One approach to such a generalization would be to approximate a conductor having an arbitrary cross section by a union of disjoint segments having rectangular cross sections. The practical difficulty with this approach is that it requires a large number of segments to obtain a reasonable approximation of the conductor cross sections. Storage requirements for the matrix Z of Eq. (15) soon would exceed available memory. Another approach is to admit conductors whose perimeters are arbitrary polygons. The conductors can then be divided into segments whose cross sections are triangles. The difficulty with this approach is that the fourfold integral in Eq. (5) cannot be evaluated in closed form, so that a costly numerical evaluation is necessary. Similarly, the evaluation of the integrals in Eq. (5) is a major obstacle to the introduction of conductors with circular cross sections.

Experimental verification

Inductance and resistance measurements were made on a large-scale model of a single stripline and also of two coupled striplines. The results of the measurements were compared with calculated values based on the theory described above.

The model, a simplified drawing of which is shown in Fig. 4, consists of first one and then two striplines placed over a ground plane. The ground plane has tabs attached to each end. The end tabs are connected to the striplines by cylindrical shorting pieces. The striplines, ground plane, end tabs, and shorting pieces are all made of brass having a measured resistivity of $1.231 \times 10^{-6}~\Omega$ -cm. Mechanical support of the striplines is provided by dielectric supporting rods. The main frame supporting the whole structure is made of aluminum. The pertinent dimensions of the model are given in Table 1.

The frequencies at which measurements were made were determined by the range of the impedance bridge

available for the experiment. With the frequency range fixed, the model dimensions were chosen so that the measured resistance would fall above the dc value but below those values which show a dependence proportional to the square root of frequency, a range not covered by existing theoretical formulas.

Inductance and resistance measurements were made using a Boonton Model 63H impedance bridge (Boonton Electronics Corp., Parsippany, NJ). The specified accuracy of the bridge in the frequency range from 5 kHz to 500 kHz, in which the measurements were made, is 0.01% + 0.2 nH for inductance and 3% + 0.000252 Ω for resistance. The accuracy of the frequency setting is +3% with a stability of 0.1%. The leads from the bridge to the stripline were brought in at right angles to the latter, as shown in Fig. 4, to eliminate inductive mutual coupling. The shorting piece at the driving end consisted of two pieces separated by an air gap at the center. The upper lead from the bridge was attached to the shorting piece at a distance $H_4/3$ from the stripline. The lower lead was attached at a distance $H_4/3$ above the end tab.

Self-inductance and resistance measurements were made before the second stripline and its shorting pieces were mounted on the apparatus. Three sets of measurements were required to determine the inductance and resistance of the part of the circuit formed by the stripline, ground plane, and end tabs.

The first measurement was to determine the inductance and resistance of the shorting pieces. A square loop of wire having perimeter P was constructed [Fig. 5(a)], and its impedance Z_1 was measured. Next, a section of wire of length H_4 was removed and was replaced with one of the shorting pieces [Fig. 5(b)], and the impedance of the new loop Z_2 was measured. The impedance of the shorting piece Z_S is then

$$Z_{\rm S} = Z_{\rm 2} - Z_{\rm 1} \left(1 - \frac{H_{\rm 4}}{P} \right),$$
 (27)

assuming that the sides of the squares are sufficiently separated so that their mutual inductance is negligible compared with their self-inductance.

The second measurement was to determine the impedance of the leads from the bridge to the split shorting piece at the left end of the line (Fig. 4). The leads and the shorting piece were disconnected from the apparatus. The shorting piece was then used to short out the leads while maintaining a separation of $H_4/3$ between the leads. The measured impedance Z_3 was the impedance of the leads Z_L plus one third the impedance Z_S of a full length of a shorting piece. Thus,

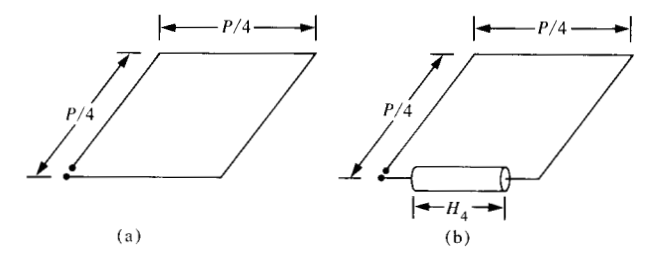


Figure 5 Determination of shorting piece impedance: (a) square wire loop with perimeter P; (b) wire loop with section of length H_A replaced with shorting piece.

$$Z_{\rm L} = Z_{\rm 3} - \frac{Z_{\rm S}}{3} \,. \tag{28}$$

The third measurement was made with the apparatus connected as shown in Fig. 4, except that the second stripline and its shorting pieces were absent. Let Z_4 be the measured impedance. Then,

$$Z = R + \hat{j}\omega L = Z_4 - Z_L - \frac{5}{3}Z_S$$
 (29)

is the impedance belonging to the stripline, ground plane, and two end tabs. The real functions R and L are, respectively, the corresponding resistance and inductance.

The measured values of L and the value calculated from the theory described earlier are listed in Table 2 and plotted on a semilog scale in Fig. 6. The calculations were made with the stripline cross section divided into 180 segments (20 divisions along its width and nine along its thickness) and the ground plane divided into 120 segments (40 along its width and three along its thickness). Separate calculations of impedance per unit length were made for the part of the stripline over the ground plane and the part of the line over the end tabs. The results were multiplied by the appropriate line lengths and added to obtain the results in Table 2. Finer subdivisions of the conductors did not significantly alter the calculated values of L. With the exception of the value at 10 kHz, the measured and calculated values of L agree to within less than 1% over the frequency range from 5 kHz to 500 kHz.

The measured and calculated values of R are listed in Table 3 and plotted on a log-log scale in Fig. 7. The difference between the measured and the calculated values was reasonably small at low frequencies but increased rapidly as the frequency increased. Furthermore, convergence of the calculation of R was very slow as the number of segments into which the conductors were divided was increased. An increase in the total number of segments from 300 to 660 only reduced the difference be-

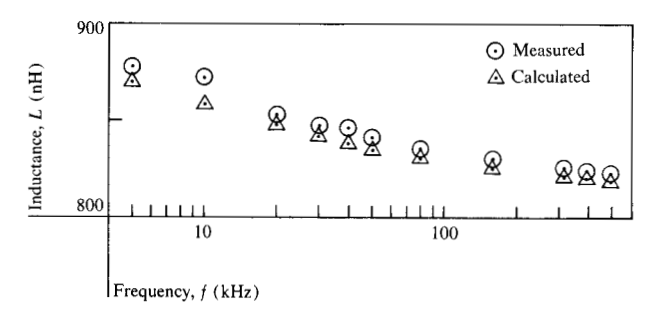


Figure 6 Measured and calculated self-inductance.

Table 2 Measured and calculated values of self-inductance L.

Frequency (kHz)	Inductance		
	Measured (nH)	Calculated (nH)	Difference (%)
5	877.6	870.1	0.85
10	873.7	858.9	1.69
20	853.4	848.5	0.57
30	848.2	842.8	0.63
40	847.2	839.0	0.97
50	841.2	836.4	0.57
80	836.0	831.7	0.51
160	831.1	826.2	0.59
320	825.3	821.9	0.41
400	824.2	820.8	0.41
500	823.2	819.8	0.41

tween measured and computed values of R at 300 kHz from 20% to 16%. The values of L, however, were not changed significantly. That L can be calculated much more accurately than R for a given division of the conductors into segments is not surprising, since L is bounded with increasing frequency, while R increases without bound.

It is interesting to compare the measured values of R with those given by published formulas for the high-frequency limit. Pucel, Masse, and Hartwig [10, 11] have derived the formula

$$R = \frac{R_{\rm S}}{\pi h} \left[1 - \left(\frac{w'}{4h} \right)^2 \right] \left[1 + \frac{h}{w'} + \frac{h}{\pi w'} \left(\ln \frac{2h}{t} - \frac{t}{h} \right) \right], (30)$$

where

$$R_{\rm S} = (\pi f \rho \mu_0)^{1/2}$$

and

$$w' = w + \frac{t}{\pi} \left(1 + \ln \frac{2h}{t} \right)$$

for the resistance per unit length of a stripline of width w and thickness t placed at a height h above a ground plane, provided that $1/2\pi < w'/h \le 2$.

Applying Eq. (30) first with $h = H_4 + T_3$ and then with $h = H_4$, one finds that

$$R_2 = 8.9823 \times 10^{-6} \sqrt{f} \ \Omega/\text{cm}$$

and

$$R_0 = 8.7476 \times 10^{-6} \sqrt{f} \ \Omega/\text{cm}$$

respectively, for the parts of the stripline over the ground plane and those over the end tabs. The total resistance is then

$$R = R_{2}L_{2} + 2R_{3}L_{3} = 1.1299 \times 10^{-3}\sqrt{f} \Omega, \tag{31}$$

where f is given in kHz. Equation (31) yields $2.5265 \times 10^{-3} \Omega$ at 5 kHz (36% below the measured values) and $2.5265 \times 10^{-2} \Omega$ at 500 kHz (17% below the measured values). The dc resistance, $R = 3.065 \times 10^{-3} \Omega$, and the resistance calculated from Eq. (31) are plotted in Fig. 7 for easy comparison with the measured results and the numerically computed results. Equation (31) coincides with the numerically calculated resistance at 160 kHz and gives a slightly better approximation for higher frequencies.

In order to measure mutual inductance, the second stripline and its two shorting pieces are installed to form a shorted secondary circuit, as shown in Fig. 4. Let Z_5 be the impedance measured with the bridge connected as shown in Fig. 4. Then

$$L_r = \operatorname{Im} (Z_{\scriptscriptstyle 5} - Z_{\scriptscriptstyle 1})/\omega \tag{32}$$

is the inductance of the primary in the presence of the shorted secondary. In Eq. (32), $Z_{\rm L}$ is the known impedance of the leads from the bridge. To extract the mutual inductance between primary and secondary circuits, it is necessary also to know the self-inductance $L_{\rm 0}$ of the primary in the presence of an open secondary. For the 5.08cm line separation used in this experiment, $L_{\rm 0}$ is not measurably different from the self-inductance of the primary circuit in the absence of the secondary circuit. Thus,

$$L_0 = \operatorname{Im} (Z_4 - Z_1)/\omega, \tag{33}$$

where Z_4 is the measured impedance used in Eq. (29).

Consider again the apparatus connected with the shorted secondary circuit in place as shown in Fig. 4. Let V_1 be the voltage drop between the leads from the bridge at their point of contact on the two halves of the split shorting piece. Let I_1 and I_2 , respectively, be the primary and secondary currents. Then, since the primary and secondary circuits are identical,

$$V_{1} = L_{0}\dot{I}_{1} + M_{0}\dot{I}_{2}, \tag{34}$$

$$0 = M_o \dot{I}_1 + L_o \dot{I}_2, \tag{35}$$

where M_0 is the mutual inductance between primary and secondary. Using Eq. (35) to eliminate \dot{I}_2 from Eq. (34), one obtains

$$V_{1} = L_{x}\dot{I}_{1} = \left(L_{0} - \frac{M_{0}^{2}}{L_{0}}\right)\dot{I}_{1},\tag{36}$$

or, solving for M,

$$M_{0} = \sqrt{L_{0}(L_{0} - L_{x})}. (37)$$

The mutual inductance M_0 obtained from Eq. (37) contains a small contribution ΔM due to the mutual coupling between the shorting pieces. There does not appear to be an easy way to measure ΔM . Fortunately, formulas exist which permit the calculation of the contribution to the mutual inductance due to the shorting pieces. Since the geometric mean distance between two parallel circular cylinders is equal to the distance between their centers, the shorting pieces can be replaced by current filaments along their centers. Then, formulas from the collection by Grover [12] can be used to calculate the contribution to mutual inductance.

For two parallel filaments of equal length x and center-to-center distance y, placed so that the end points of one filament have coordinates (0, 0) and (x, 0) and those of the other have (0, y) and (x, y), Grover gives the formula

$$m(x, y) = 2x \left[\ln \left(\frac{x}{y} + \sqrt{1 + \left(\frac{x}{y} \right)^2} \right) - \sqrt{1 + \left(\frac{y}{x} \right)^2 + \frac{y}{x}} \right].$$

$$(38)$$

For two filaments, one of length x and the other of x/3, with center-to-center spacing y, placed so that the coordinates of the end points of the first are (0, 0) and (x, 0) and those of the end points of the second are (0, y) and (x/3, y), Grover gives

$$m'(x, y) = \frac{1}{2} [m(x, y) + m(x/3, y) - m(2x/3, y)],$$
 (39)

where m(x, y) is given by Eq. (38). The contribution ΔM to the mutual inductance M_0 due to the shorting pieces is then

$$\Delta M = m(H_4, S_1) + 2m'(H_4, S_1) = 5.51 \text{ nH}.$$
 (40)

The part of the mutual inductance attributable strictly to the striplines, the ground plane, and the end tabs is then

$$M = M_0 - \Delta M, \tag{41}$$

where M_0 is given by Eq. (37) and ΔM by Eq. (40).

The measured and calculated values of M are listed in Table 4 and plotted on a semilog scale in Fig. 8. The mea-

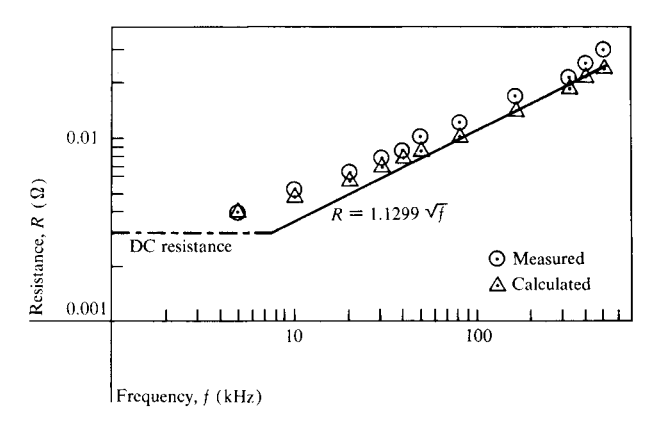


Figure 7 Measured and calculated resistance.

Table 3 Measured and calculated values of resistance R.

Frequency (kHz)	Resistance			
	Measured (Ω)	Calculated (Ω)	Difference (%)	
5	3.97×10^{-3}	4.02×10^{-3}	-1.26	
10	4.94×10^{-3}	4.75×10^{-3}	3.85	
20	6.47×10^{-3}	6.01×10^{-3}	7.11	
30	7.86×10^{-3}	7.09×10^{-3}	9.80	
40	8.40×10^{-3}	7.99×10^{-3}	4.88	
50	9.98×10^{-3}	8.77×10^{-3}	12.12	
80	1.198×10^{-2}	1.058×10^{-2}	11.69	
160	1.693×10^{-2}	1.428×10^{-2}	15.65	
320	2.154×10^{-2}	1.962×10^{-2}	8.91	
400	2.560×10^{-2}	2.182×10^{-2}	14.76	
500	3.040×10^{-2}	2.430×10^{-2}	20.06	

sured values of M are extracted from the measured values of L_0 and L_r by means of Eqs. (37), (40), and (41). The calculated values were obtained by calculating the mutual inductance per unit length for the sections of striplines over the ground plane and for those over the end tabs, multiplying the results by the appropriate lengths and adding them together to obtain the final results in Table 4 and Fig. 8. Since mutual inductance is a much less sensitive function of current distribution than self-inductance or resistance, convergence was obtained with the striplines divided into 40 segments each (eight along the width and five along the thickness), and the ground plane and the end tabs divided into 90 segments (30 along the width and three along the thickness). With the exception of the value at 10 kHz, the measured and calculated values agree to within 2%.

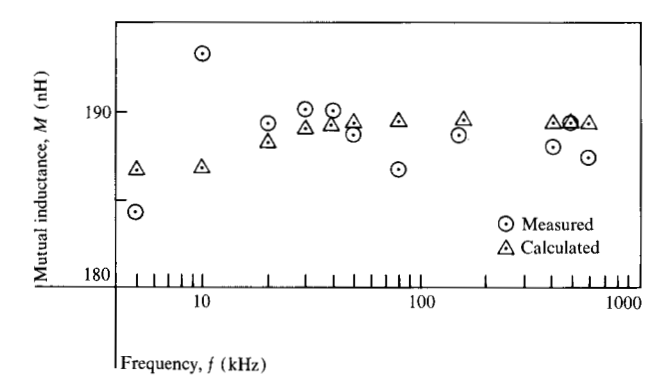


Figure 8 Measured and calculated mutual inductance.

Table 4 Measured and calculated values of mutual inductance M.

Frequency (kHz)	Mutual inductance			
	Measured (nH)	Calculated (nH)	Difference (%)	
5	184.4	186.89	-1.35	
10	193.4	186.89	3.37	
20	189.4	188.44	0.51	
30	190.1	189.03	0.56	
40	190.0	189.27	0.38	
50	188.6	189.39	-0.42	
80	186.7	189.52	-1.51	
160	188.5	189.53	-0.54	
320	188.1	189.44	-0.69	
400	189.5	189.41	0.05	
500	187.4	189.37	-1.05	

Conclusions

A simple network model has been proposed for calculating the frequency-dependent inductances and resistances per unit length for multiconductor transmission lines. When restricted to conductors having rectangular cross sections, numerical computation is feasible on present-day computer systems.

A comparison has been made between calculated results and measurements made on a large-scale model of one and two striplines over a ground plane. A reasonable rate of convergence was observed with respect to the number of segments into which conductors were subdivided, and very accurate results were obtained for both self- and mutual inductance. A slower convergence and poorer results were obtained for resistance, especially at the higher frequencies. The computations, though

lengthy, are of a reasonable magnitude. The calculations using 300 segments, for example, required 500 000 bytes of memory and slightly less than 1.5 minutes per frequency on an IBM System 370/168.

The extremely large number of segments required to obtain accurate resistance values at high frequencies is troublesome, but is not an insurmountable difficulty. Accuracy can be improved by using the formulas of Pucel, Masse, and Hartwig, e.g., Eq. (30), to calculate resistance whenever these formulas yield a resistance higher than the numerically computed value.

References

- H. B. G. Casimir and J. Ubbink, "The Skin Effect," Phillips Tech. Rev. 28, 271-283, 300-315, 366-381 (1967).
- P. Silvester, "Model Network Theory of Skin Effect in Flat Conductors," Proc. IEEE 59, 1147-1151 (1966).
- B. D. Popović and Z. M. Popović, "Method of Determining Power-Frequency Current Distributions in Cylindrical Conductors," Proc. IEE 119, 569-574 (1972).
- B. D. Popović and D. N. Filipović, "Theory of Power-Frequency Proximity Effect for Strip Conductors," *Proc. IEE* 122, 839-842 (1975).
- P. Graneau, "Alternating and Transient Conduction Currents in Straight Conductors of any Cross-Section," Intl. J. Electron. 19, 41-59 (1965).
- Electron. 19, 41-59 (1965).
 6. P. Graneau, "Computation of Losses and Inter-conductor Forces in Low-temperature A.C. Power Circuits," Intl. J. Electron. 22, 1-18 (1967).
- A. E. Ruehli, "Inductance Calculations in a Complex Integrated Circuit Environment," IBM J. Res. Develop. 16, 470-481 (1972).
- A. E. Ruehli, "Equivalent Circuit Models for Three-Dimensional Multiconductor Systems," *IEEE Trans. Microwave Theory Tech.* MTT-22, 216-221 (1974).
- A. E. Ruehli, N. Kulasza, and J. Pivnichny, "Inductance of Nonstraight Conductors Close to a Ground Return Plane," *IEEE Trans. Microwave Theory Tech.* MTT-23, 706-708 (1975).
- R. A. Pucel, D. J. Masse, and C. P. Hartwig, "Losses in Microstrip," *IEEE Trans. Microwave Theory Tech.* MTT-16, 342-350 (1968).
- R. A. Pucel, D. J. Masse, and C. P. Hartwig, correction to "Losses in Microstrip," *IEEE Trans. Microwave Theory Tech.* MTT-16, 1064 (1968).
- 12. F. W. Grover, *Inductance Calculations, Working Formulas, and Tables*, Dover Publications, New York, 1962, p. 31, Eq. (1) and p. 46, Eq. (32).

Received March 20, 1979; revised June 25, 1979

W. T. Weeks, L. L. Wu, and M. F. McAllister are located at the IBM Data Systems Division laboratory, East Fish-kill (Hopewell Junction), New York 12533. A. Singh is located at Southern University, Baton Rouge, Louisiana 70813.